Research Article | Vol. 24, No. 16 | 8 Aug 2016 | OPTICS EXPRESS 18399

Optics EXPRESS

High-quality-factor planar optical cavities with laterally stopped, slowed, or reversed light

STEVEN J. BYRNES,[1,2] MOHAMMADREZA KHORASANINEJAD,[1] AND FEDERICO CAPASSO[1,*]

[1]*Harvard John A. Paulson School of Engineering and Applied Sciences, Cambridge, Massachusetts, USA*
[2]*Current address: Charles Stark Draper Laboratory, Cambridge, Massachusetts, USA*
[*]*capasso@seas.harvard.edu*

Abstract: In a planar optical cavity, the resonance frequencies increase as a function of in-plane wavevector according to a standard textbook formula. This has well-known consequences in many different areas of optics, from the shifts of etalon peaks at non-normal angles, to the properties of transverse modes in laser diodes, to the effective mass of microcavity photons, and so on. However, this standard formula is valid only when the reflection phase of each cavity mirror is approximately independent of angle. There is a certain type of mirror—a subwavelength dielectric grating near a guided mode resonance—with not only a strongly angle-dependent reflection phase, but also very high reflectance and low losses. Simulations show that by using such mirrors, high-quality-factor planar cavities can be designed that break all these textbook rules, leading to resonant modes that are slow, stopped or even backward-propagating in the in-plane direction. In particular, we demonstrate experimentally high-Q planar cavities whose resonance frequency is independent of in-plane wavevector—i.e., the resonant modes have zero in-plane group velocity, for one polarization but both in-plane directions. We discuss potential applications in various fields including lasers, quantum optics, and exciton-polariton condensation.

OCIS codes: (140.4780) Optical resonators; (140.3410) Laser resonators; (270.0270) Quantum optics.

References and links

1. E. Hecht, *Optics*, 4th ed. (Addison Wesley, 2002).
2. A. V. Kavokin, J. J. Baumberg, G. Malpuech, and F. P. Laussy, *Microcavities* (Oxford University, 2007).
3. M. A. Kats, R. Blanchard, P. Genevet, and F. Capasso, "Nanometre optical coatings based on strong interference effects in highly absorbing media," Nat. Mater. **12**(1), 20–24 (2012).
4. S. Boutami, B. Ben Bakir, X. Letartre, J. L. Leclercq, and P. Viktorovitch, "Photonic crystal slab mirrors for an ultimate vertical and lateral confinement of light in vertical Fabry Perot cavities," Proc. SPIE **6989**, 69890V (2008).
5. S. Mukherjee, A. Spracklen, D. Choudhury, N. Goldman, P. Öhberg, E. Andersson, and R. R. Thomson, "Observation of a localized flat-band state in a photonic Lieb lattice," Phys. Rev. Lett. **114**(24), 245504 (2015).
6. S. Flach, D. Leykam, J. D. Bodyfelt, P. Matthies, and A. S. Desyatnikov, "Detangling flat bands into Fano lattices," Europhys. Lett. **105**(3), 30001 (2014).
7. M. Ibanescu, M. Soljacic, S. G. Johnson, and J. D. Joannopoulos, "Ultra-flat bands in two-dimensional photonic crystals," Proc. SPIE **6128**, 612808 (2006).
8. H. Takeda, T. Takashima, and K. Yoshino, "Flat photonic bands in two-dimensional photonic crystals with kagome lattices," J. Phys. Condens. Matter **16**(34), 6317–6324 (2004).
9. K. Staliunas and R. Herrero, "Nondiffractive propagation of light in photonic crystals," Phys. Rev. E Stat. Nonlin. Soft Matter Phys. **73**(1), 016601 (2006).
10. K. L. Tsakmakidis, A. D. Boardman, and O. Hess, "'Trapped rainbow' storage of light in metamaterials," Nature **450**(7168), 397–401 (2007).
11. R. Yang, W. Zhu, and J. Li, "Realization of "trapped rainbow" in 1D slab waveguide with surface dispersion engineering," Opt. Express **23**(5), 6326–6335 (2015).
12. K. Staliunas, O. Egorov, Y. S. Kivshar, and F. Lederer, "Bloch cavity solitons in nonlinear resonators with intracavity photonic crystals," Phys. Rev. Lett. **101**(15), 153903 (2008).
13. J. L. Zhang, W. D. Shen, P. Gu, Y. G. Zhang, H. T. Jiang, and X. Liu, "Omnidirectional narrow bandpass filter based on metal-dielectric thin films," Appl. Opt. **47**(33), 6285–6290 (2008).

#267769 http://dx.doi.org/10.1364/OE.24.018399
Journal © 2016 Received 20 Jun 2016; revised 22 Jul 2016; accepted 25 Jul 2016; published 2 Aug 2016

Optics EXPRESS

14. B. J. M. Hausmann, B. J. Shields, Q. Quan, Y. Chu, N. P. de Leon, R. Evans, M. J. Burek, A. S. Zibrov, M. Markham, D. J. Twitchen, H. Park, M. D. Lukin, and M. Loncar, "Coupling of NV centers to photonic crystal nanobeams in diamond," Nano Lett. **13**(12), 5791–5796 (2013).
15. J. S. Q. Liu and M. L. Brongersma, "Omnidirectional light emission via surface plasmon polaritons," Appl. Phys. Lett. **90**(9), 091116 (2007).
16. T. Byrnes, N. Y. Kim, and Y. Yamamoto, "Exciton-polariton condensates," Nat. Phys. **10**(11), 803–813 (2014).
17. Z. Wang, B. Zhang, and H. Deng, "Dispersion engineering for vertical microcavities using subwavelength gratings," Phys. Rev. Lett. **114**(7), 073601 (2015).
18. J.-H. Jiang and S. John, "Photonic crystal architecture for room-temperature equilibrium Bose-Einstein condensation of exciton polaritons," Phys. Rev. X **4**(3), 031025 (2014).
19. F. Baboux, L. Ge, T. Jacqmin, M. Biondi, E. Galopin, A. Lemaître, L. Le Gratiet, I. Sagnes, S. Schmidt, H. E. Türeci, A. Amo, and J. Bloch, "Bosonic condensation and disorder-induced localization in a flat band," Phys. Rev. Lett. **116**(6), 066402 (2016).
20. Y.-C. Cheng and K. Staliunas, "Negative Goos-Hänchen shift in reflection from subwavelength gratings," J. Nanophotonics **8**(1), 084093 (2014).
21. R. H. Renard, "Total reflection: A new evaluation of the Goos-Hänchen shift," J. Opt. Soc. Am. **54**(10), 1190 (1964).
22. H. Shin, M. F. Yanik, S. Fan, R. Zia, and M. L. Brongersma, "Omnidirectional resonance in a metal–dielectric–metal geometry," Appl. Phys. Lett. **84**(22), 4421–4423 (2004).
23. J.-W. Dong, K.-S. Wu, C. Mu, and H.-Z. Wang, "Multiple omnidirectional resonances in a metamaterial sandwich," Phys. Lett. A **372**(24), 4532–4535 (2008).
24. Y.-H. Chen, J.-W. Dong, and H.-Z. Wang, "Conditions of near-zero dispersion of defect modes in one-dimensional photonic crystals containing negative-index materials," J. Opt. Soc. Am. B **23**(4), 776–781 (2006).
25. Y. H. Chen, J. W. Dong, and H. Z. Wang, "Omnidirectional resonance modes in photonic crystal heterostructures containing single-negative materials," J. Opt. Soc. Am. B **23**(10), 2237–2240 (2006).
26. A. Hosseini and Y. Massoud, "Optical range microcavities and filters using multiple dielectric layers in metal-insulator-metal structures," J. Opt. Soc. Am. A **24**(1), 221–224 (2007).
27. P. Viktorovitch, B. Ben Bakir, S. Boutami, J. L. Leclercq, X. Letartre, P. Rojo-Romeo, C. Seassal, M. Zussy, L. Di Cioccio, and J. M. Fedeli, "3D harnessing of light with 2.5D photonic crystals," Laser Photonics Rev. **4**(3), 401–413 (2010).
28. S. M. Norton, T. Erdogan, and G. M. Morris, "Coupled-mode theory of resonant-grating filters," J. Opt. Soc. Am. A **14**(3), 629–639 (1997).
29. R. Magnusson, M. Shokooh-Saremi, K. J. Lee, J. Curzan, D. Wawro, S. Zimmerman, W. Wu, J. Yoon, H. G. Svavarsson, and S. H. Song, "Leaky-mode resonance photonics: an applications platform," Proc. SPIE **8102**, 810202 (2011).
30. P. Vincent and M. Nevière, "Corrugated dielectric waveguides: A numerical study of the second-order stop bands," Appl. Phys. (Berl.) **20**(4), 345–351 (1979).
31. E. Popov, L. Mashev, and D. Maystre, "Theoretical study of the anomalies of coated dielectric gratings," Opt. Acta Int. J. Opt. **33**(5), 607–619 (1986).
32. D. Maystre, "Theory of Wood's Anomalies," in *Plasmonics: From Basics to Advanced Topics*, S. Enoch and N. Bonod, eds. (Springer, 2012), p. 39.
33. J. He, J. Yi, and S. He, "Giant negative Goos-Hänchen shifts for a photonic crystal with a negative effective index," Opt. Express **14**(7), 3024–3029 (2006).
34. R. Yang, W. Zhu, and J. Li, "Giant positive and negative Goos-Hänchen shift on dielectric gratings caused by guided mode resonance," Opt. Express **22**(2), 2043–2050 (2014).
35. T. Tamir and H. L. Bertoni, "Lateral displacement of optical beams at multilayered and periodic structures," J. Opt. Soc. Am. **61**(10), 1397 (1971).
36. A. M. Shaltout, A. V. Kildishev, and V. M. Shalaev, "Compact subwavelength cavities using reflecting metasurfaces," in *2014 Conference on Lasers and Electro-Optics (CLEO) - Laser Science to Photonic Applications* (2014), pp. 1–2.
37. K. Staliunas, M. Peckus, and V. Sirutkaitis, "Sub- and superdiffractive resonators with intracavity photonic crystals," Phys. Rev. A **76**(5), 051803 (2007).
38. M. Peckus, R. Rogalskis, M. Andrulevicius, T. Tamulevicius, A. Guobiene, V. Jarutis, V. Sirutkaitis, and K. Staliunas, "Resonators with manipulated diffraction due to two- and three-dimensional intracavity photonic crystals," Phys. Rev. A **79**(3), 033806 (2009).
39. R. Iliew, C. Etrich, T. Pertsch, F. Lederer, and K. Staliunas, "Subdiffractive all-photonic crystal Fabry-Perot resonators," Opt. Lett. **33**(22), 2695–2697 (2008).
40. M. Shokooh-Saremi and R. Magnusson, "Leaky-mode resonant reflectors with extreme bandwidths," Opt. Lett. **35**(8), 1121–1123 (2010).
41. C. J. Chang-Hasnain and W. Yang, "High-contrast gratings for integrated optoelectronics," Adv. Opt. Photonics **4**(3), 379–440 (2012).
42. V. Liu and S. Fan, "S^4: a free electromagnetic solver for layered periodic structures," Comput. Phys. Commun. **183**(10), 2233–2244 (2012).
43. M. Khorasaninejad, N. Abedzadeh, J. Walia, S. Patchett, and S. S. Saini, "Color matrix refractive index sensors using coupled vertical silicon nanowire arrays," Nano Lett. **12**(8), 4228–4234 (2012).

Optics EXPRESS

44. M. A. Kats, D. Woolf, R. Blanchard, N. Yu, and F. Capasso, "Spoof plasmon analogue of metal-insulator-metal waveguides," Opt. Express **19**(16), 14860–14870 (2011).
45. F. Aieta, P. Genevet, M. A. Kats, N. Yu, R. Blanchard, Z. Gaburro, and F. Capasso, "Aberration-free ultrathin flat lenses and axicons at telecom wavelengths based on plasmonic metasurfaces," Nano Lett. **12**(9), 4932–4936 (2012).
46. N. Yu and F. Capasso, "Flat optics with designer metasurfaces," Nat. Mater. **13**(2), 139–150 (2014).

1. Motivation and theory

Two plane-parallel mirrors set up an optical cavity with a series of resonant frequencies, which generally shift when the in-mirror-plane wavevector is changed—for example, by sending light into the cavity at an angle tilted away from normal incidence. This shift in resonant frequency is quantified by the following simple argument, which can be found in basic optics textbooks [1]. Cavity resonances occur when the round-trip phase shift of light is an integer multiple of 2π. If the mirrors are in the x-y plane, the resonances satisfy $2nLk_z = 2\pi m + \varphi$, where n is the refractive index inside the cavity, L is the cavity length, k_z is the z-component of the wavevector for the m'th cavity resonance, and φ is an offset related to reflection phase shifts. The important aspect of this formula is that a resonance's k_z does not (explicitly) depend on the other components of the wavevector $\mathbf{k}_{xy} = (k_x,k_y)$. By combining this observation with the formula relating wavevector to frequency, $\omega^2 = (c/n)^2(k_z^2 + |\mathbf{k}_{xy}|^2)$, we will have:

$$\omega_{\mathrm{res},m}\left(\mathrm{k}_{xy}\right) = \left[\omega_{\mathrm{res},m}(0)^2 + \left(c\left|\mathrm{k}_{xy}\right|/n\right)^2\right]^{1/2} = \omega_{\mathrm{res},m}\left(0\right)/\cos\theta, \qquad (1)$$

where c is the speed of light, $\omega_{\mathrm{res},m}$ is the frequency of the m'th cavity resonance, $\theta = \tan^{-1}(|\mathbf{k}_{xy}| / k_z)$ is the light propagation angle inside the cavity with respect to the normal, and $\omega_{\mathrm{res},m}(0)$ is the resonant frequency for $\theta = |\mathbf{k}_{xy}| = 0$, e.g. if light enters the cavity normal to the mirrors.

This standard Eq. (1) has many manifestations from the widespread application of planar optical cavities. For Fabry-Pérot etalons, the rule says that transmission peaks should blue-shift as the etalon is tilted away from normal. For laser diodes, it predicts that higher-order transverse modes (which are built out of larger $\mathbf{k}_{xy}$) should have higher frequency than the fundamental mode. For planar microcavities, it implies that the photon effective mass should be positive [2].

Despite the widespread use of this standard formula (1), it is not universally valid, as it is relies on the assumption that the reflection phase at the mirrors is independent of θ and ω. This is usually a very good approximation. For example, a metal mirror has a reflection phase shift $\approx\pi$ for any incidence angle, unless it is very lossy [3], but very lossy mirrors are not suitable for high-Q cavities. Similarly, interfaces between lossless dielectric materials have reflection phases of either 0 or π, except for the case of total internal reflection (TIR), but TIR does not occur for planar cavities near normal incidence. On the other hand, for certain kinds of reflectors, as discussed in the next section, the reflection phase can depend strongly on angle, and hence Eq. (1) will be violated. For example, when a cavity resonance ω_{res} is independent of $\mathbf{k}_{xy}$, we can say this resonance has *laterally-stopped light*, since there is zero in-plane group velocity: $\partial\omega_{\mathrm{res}}/\partial k_x = \partial\omega_{\mathrm{res}}/\partial k_y = 0$. Similarly, when ω_{res} decreases with $|\mathbf{k}_{xy}|$, we can say that the cavity resonance is *laterally reverse-propagating* (negative group velocity).

We particularly focus on a planar vertical cavity with a high-Q (quality factor) laterally-stopped-light resonance—where ω_{res} is independent of $\mathbf{k}_{xy}$ for at least one polarization—and which has a very large mirror surface area compared to the wavelength. Such a cavity would have a continuum of high-Q modes with different $\mathbf{k}_{xy}$, but they would all be degenerate in frequency. Therefore, any arbitrary complex superposition of those modes would also be a stable, high-Q cavity mode. In particular, as shown in Fig. 1(a), a localized mode would be a stable resonance—it would *not* spread out laterally, despite the lack of curved mirrors, index gradients, or any other traditional method of light confinement. This flat-band lateral

Optics EXPRESS

confinement effect [4–9] can be understood in at least two additional ways. First, the light does not spread because the in-plane group velocity $\partial\omega_{res}/\partial\mathbf{k}_{xy}$ is zero. Second, Fig. 1(b) shows a ray-optics picture, in which the angle-dependent reflection phase at the top mirror creates a negative Goos–Hänchen shift $\mathbf{s} = \partial\varphi_{reflection}/\partial\mathbf{k}_{xy}$, which cancels any lateral motion [4,10,11]. In Visualization 1, we show a simulated movie of this effect. (This discussion assumes linear optics; at higher intensity, nonlinearity may cause a richer variety of mode dynamics [12].)

Figure 1(c) shows this same cavity used as a Fabry-Pérot etalon. This has the narrow-band filtering and field-enhancing properties of a traditional etalon, but it works regardless of the shape of the incoming wavefront [13]. Figure 1(d) suggests one potential application in quantum optics. Quantum optics experiments often require a laborious procedure or trial-and-error approach to place a quantum emitter (e.g. an atom) in the same location as a localized high-Q optical mode (e.g. a photonic crystal defect mode) [14]. However, in this planar cavity, an emitter at any location on the sheet has its own localized optical mode with Purcell-enhanced light-matter coupling [15]. Thus there is no need to bring the emitter to a special location. This simplifies the experimental setup—particularly for quantum computing applications which might involve thousands of cavity-coupled quantum emitters. Finally, Fig. 1(e) puts these cavities in the context of planar microcavity theory [2]. The variation of ω_{res} with $|\mathbf{k}_{xy}|$ is parametrized by a "photon effective mass", which is positive in conventional cavities that follow Eq. (1). The cavities described in this work (see Figs. 3(a)-3(c) below) can have larger, or infinite, or negative photon effective mass. The ability to engineer the effective mass of a microcavity may help achieve exciton-polariton condensation [2,16,17], as the band structure directly impacts scattering rates, condensation temperature, the "polariton bottleneck", and so on [2,18,19].

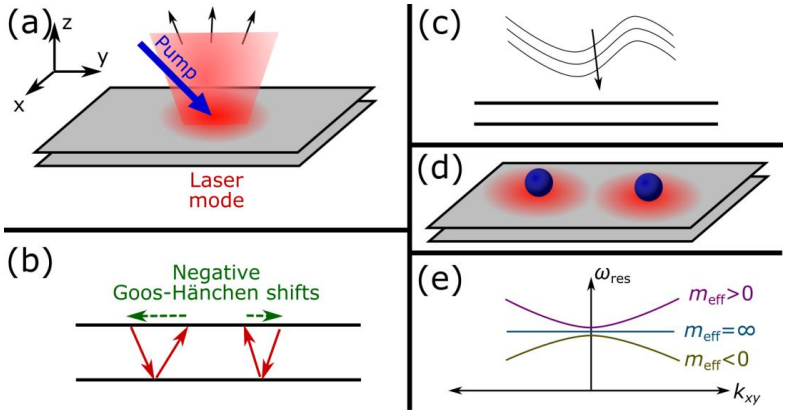

Fig. 1. **(a)** In a laser cavity with a laterally-stopped-light resonance (ω_{res} independent of $\mathbf{k}_{xy}$, so the in-plane group velocity $\partial\omega_{res}/\partial k_x = \partial\omega_{res}/\partial k_y = 0$), there are a large number of degenerate modes, including localized modes. These localized modes do not spread out, despite the absence of curvature or any other in-plane light guiding. For example, with a localized pump, the system will lase on a localized mode that best overlaps the pump [4]. Visualization 1 shows a simulated movie of this effect. **(b)** An alternative way to understand the stable localized modes is as a result of negative Goos–Hänchen shifts. **(c)** Such a cavity also acts as a Fabry-Pérot etalon that works for any incident wavefront. **(d)** If a quantum emitter such as a quantum dot is placed on such a cavity, it will have Purcell-enhanced light-matter coupling to a mode localized in its vicinity. **(e)** Microcavity theory parametrizes $\omega_{res}(\theta)$ via "photon effective mass"; we can make cavities where this parameter is positive, negative, or infinite.

2. Reflector design

Ordinary high-Q optical cavity mirrors have an approximately-fixed reflection phase regardless of incidence angle and frequency, leading to Eq. (1). What kind of reflector would violate this rule—and more specifically, violate it in such a way as to allow high-Q laterally-

Optics EXPRESS

stopped-light resonances? It turns out that there is a general requirement. If a plane wave with, say, $k_x>0$ goes towards the reflector, somewhere in the structure there must be one or more layers in which the Poynting vector points in the opposite direction, $S_x<0$. In other words, Fig. 1(b) can be taken literally, with the dashed arrow indicating energy flow [4,11,20,21]. The rationale is as follows. For laterally-stopped light, the group velocity in the *x-y* plane ($\partial\omega_{res}/\partial\mathbf{k}_{xy}$) is zero. Therefore, if we construct a finite wave packet around a certain $\mathbf{k}_{xy}$, its envelope will not move in the x-y plane. This can only happen if there is zero net energy flow in the x-y plane. So, if there are normal dielectric layers with $S_x>0$, they must be counteracted by anomalous layers with $S_x<0$. (This logic works for high-Q modes only. If the cavity lifetime is short and the wave packet is large, there can be some lateral energy flow within the wave packet as the light is escaping.)

Now one can see why conventional high-Q optical cavity mirrors are unsuitable for laterally-stopped-light cavity resonances: The situation where $S_x<0$ while $k_x>0$ cannot occur in a Bragg mirror, or indeed in any planar dielectric multilayer film. Nor can it occur in a highly-reflective metal mirror, as negligible light enters the metal ($\boldsymbol{S}\approx 0$).

This reverse energy flow *can* occur in metals or other materials with negative permittivity, negative permeability, or both; and this allows laterally-stopped-light resonances to occur [15,22–26]. The original example was a metal-insulator-metal plasmonic cavity, which can be designed in such a way that the resonant frequency is independent of incidence angle, all the way from normal incidence to 90°—a so-called "omnidirectional resonance" [15,22,26]. However, these designs require substantial optical power to be flowing in the metal or negative-index material, contributing to the absorption loss. Hence these cavities have low Q, typically $Q\lesssim 10$, making them generally unsuitable for lasers, quantum optics, exciton-polariton microcavities, or the other application areas discussed in this work.

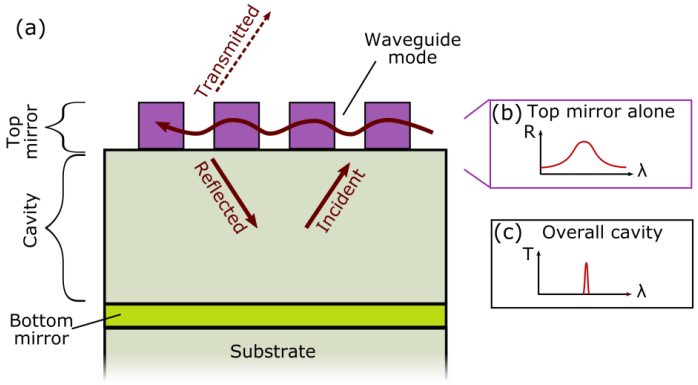

Fig. 2. **(a)** Our planar cavity has two mirrors. The bottom is a normal metal mirror. The top mirror is a resonant grating filter, i.e. a high-index grating that both supports in-plane guided modes and enables them to couple out. **(b)** At the guided mode resonance feature, the grating reflectance approaches 100%. **(c)** The two mirrors together form a cavity with a narrow cavity resonance, which sits within the broader guided mode resonance [4,27].

To gain complete control over the flow of energy in a cavity without introducing losses, we propose to use resonant grating filters [4,28,29] (Fig. 2). These filters are built from two required ingredients, although a single dielectric grating layer often provides both ingredients at once. The first ingredient is a dielectric waveguide, which supports guided modes propagating in the *x-y* plane. The second ingredient is a periodic grating structure, also in the *x-y* plane, with a small enough period that it has only a 0 (trivial) diffraction order propagating into the air and substrate, but a large enough period that it can couple the waveguide's guided modes into free space. The guided modes thus become *leaky*, and there is a resonance where the incoming light has just the right angle and frequency to couple into a

Optics EXPRESS

guided mode. There is a rapid variation in reflectance at this resonance, often with a peak reflectance value of ~100% at the center of the resonance [30,31]. In addition, the resonance is associated with a rapid change in reflection phase, by up to 2π [29,31]. This resonant grating filter effect is closely related to the classic Wood's Anomaly of metal diffraction gratings, in which diffraction efficiencies change dramatically when the grating couples light to surface plasmon polaritons [32].

A resonant grating filter satisfies all our requirements for the cavity mirror. In addition to the high reflectance (>99%) and negligible absorption losses, it can have the reverse in-plane energy flow mentioned above [4,20]. The latter arises from coupling incoming light with in-plane wavevector $\mathbf{k}_{xy,\mathrm{inc}}$ to guided modes with wavevector $\mathbf{k}_{xy,\mathrm{guided}} = \mathbf{k}_{xy,\mathrm{inc}} + \mathbf{G}$, where $\mathbf{G}$ is a grating reciprocal lattice vector. As shown in Fig. 2(a), it is quite possible for $k_{x,\mathrm{inc}} > 0$ yet $k_{x,\mathrm{guided}} < 0$. Relatedly, these structures can show strong negative Goos–Hänchen shifts [20,33–35]. Another advantageous feature of resonant grating filter mirrors is that, since the reflection phase need not be 0 or π, the cavity can be thinner than $\lambda/2n$ [36], as indeed we will see in the examples below. (Low mode volume is helpful for quantum optics.) Finally, using these mirrors leads to several practical benefits compared to some earlier related work [37–39], including a vertical-cavity design (for easy in- and out-coupling), simple monolithic growth and patterning, and absence of extra diffraction orders.

In a resonant grating filter, the resonance linewidth depends on the leakage of the guided mode. Small leakage results in a narrow reflectance peak (useful for telecommunications filtering [28]), whereas high leakage creates a broad high-reflectance feature (the basis for "high-contrast grating" reflectors [40,41]). Our application falls between these extreme cases: The grating resonance should be broad enough to create high reflectance over a reasonable range of angles and frequencies—and certainly much broader than our high-Q cavity resonance (Figs. 2(b)-2(c))—but narrow enough to get a sufficiently sharp variation in reflection phase as a function of angle.

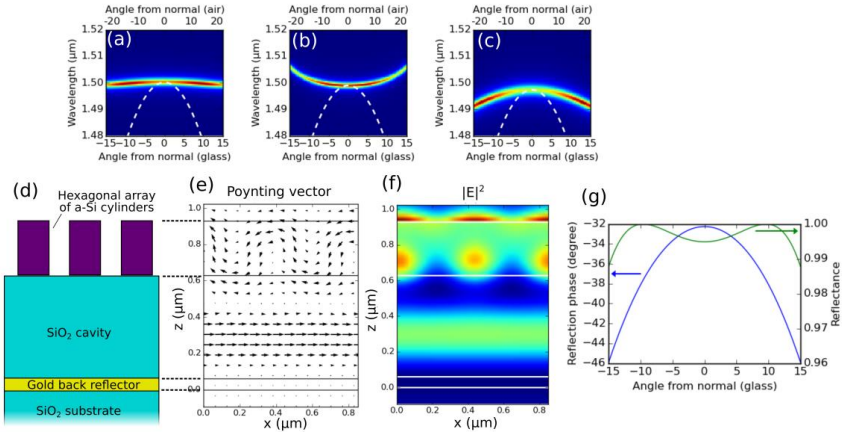

Fig. 3. **(a)-(c)** For three different cavities we designed (see Table 1 for parameters), we send in a CW plane-wave from the substrate (through the thin gold) at a given wavelength and angle. The plot shows the energy stored in the cavity, so a bright band occurs at the cavity resonance. These three cavities (a-c) show some of the possibilities, where the light in the cavity is (a) stopped, (b) reversed, or (c) slowed in the plane of the cavity. The white dashed curve is the curve we would expect from ordinary planar cavities, Eq. (1). See Fig. 5 for other polarizations and directions. **(d)** Schematic of our cavities, which use a conventional gold mirror on one side, and a hexagonal array of dielectric cylinders on the other side. For cavity (a), with 1.5μm light incident 5° from normal, we show **(e)** the Poynting vector, and **(f)** the electric field amplitude profile (both averaged over the y-coordinate pointing into the page). Although the incident light tilts rightward, the energy flows leftward in the cylinder array, giving an overall average energy flow of zero, as we expect. **(g)** Reflection phase and amplitude of just the cylinder array (i.e., leaving out the gold) for the structure (a).

Optics EXPRESS

Our reflector, constructed along these lines, consists of a hexagonal array of dielectric cylinders, with subwavelength spacing (Fig. 3(d)). This special reflector sits on one side of our planar optical cavity, with a metal mirror on the other side. In the design, we had four main adjustable parameters: dielectric cylinder height, radius, and spacing, and cavity thickness. We select the parameters so that the grating reflector has both high reflectance and the appropriate angle-vs-reflection-phase profile to create the desired cavity resonance effects, using a numerical search of the parameter space. We examined a ± 15° range of angles around normal incidence. Three example simulation results are shown in Figs. 3(a)-3(c). (The corresponding geometries are in Table 1, rows A-C respectively.) Our simulations show that full control over the energy flow is realized by these designs, including laterally-stopped light (Fig. 3(a), Q≈680-790), laterally-reversed (negative group velocity) light (Fig. 3(b), Q≈820-1000), and laterally-slow light (Fig. 3(c), Q≈450-600). All simulations were performed using Rigorous Coupled-Wave Analysis (S^4 software [42]). We checked some results with the Finite Difference Time Domain method (Lumerical, Inc.), which was also used for making a movie—Visualization 1—that demonstrates the fact that light in the stopped-light cavity of Fig. 3(a) tends not to spread out in the plane as discussed earlier.

Because of the symmetry of the hexagonal lattice, the results shown in Figs. 3(a)-3(c) are essentially independent of azimuthal angle—i.e., they depend on the magnitude of $\mathbf{k}_{xy}$, but not on its direction in the x-y plane. This is shown in the Appendix, Fig. 5. In particular, in the structure of Fig. 3(a), ω_{res} is independent of both k_x and k_y, enabling full 3D confinement of the modes, unlike earlier proposals involving 1D gratings [4,17]. Note however that these results apply to the TE (s-polarized) cavity modes only. The TM mode behavior is also shown in Fig. 5, and has a laterally-reverse-propagating resonance in all cases, i.e. ω_{res} decreasing with $|\mathbf{k}_{xy}|$.

Although these cavities were designed to have high Q-factor within ± 15° of normal incidence, the phenomena discussed above (Fig. 1) are not qualitatively affected by this restriction. For example, we can consider a cavity mode with complex amplitude $E(x,y)$ (neglecting polarization for simplicity). For this to be a high-quality-factor mode, its Fourier transform $\tilde{E}(\mathbf{k}_{xy})$ should be consist exclusively of $\mathbf{k}_{xy}$ vectors corresponding to modes which all have the same resonant frequency and which all have a high quality factor. The uncertainty principle says that if we want $E(x,y)$ to be tightly confined in real space, we need to draw from a large spread of $\mathbf{k}_{xy}$. If we can only use $\mathbf{k}_{xy}$ within 15° of normal incidence, we can still build localized modes—but they will not be quite as sharply localized as if we did not have that restriction.

To verify this theory, we experimentally demonstrated an anomalous resonant-frequency-vs-angle curve indicative of laterally-stopped light.

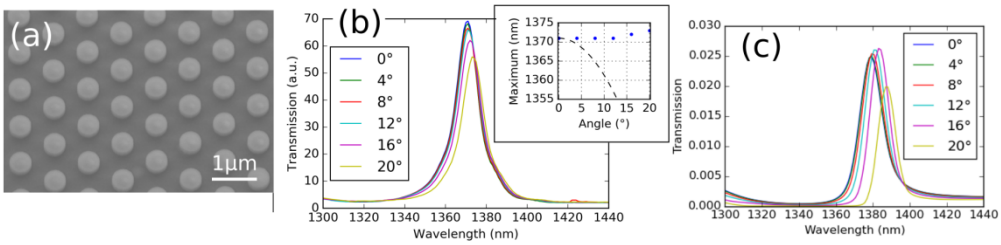

Fig. 4. **(a)** Scanning electron micrograph of the cavity, showing the array of amorphous silicon pillars. The experiments **(b)** and corresponding simulations **(c)** show a transmission peak which is almost angle-independent, but slightly decreases in frequency away from normal (opposite of conventional cavities). The indicated angle is the angle of light in air, relative to the wafer normal. The simulation parameters were based on SEM measurements of the structure, see Table 1. The inset of (b) shows the wavelength at the maximum of each curve, compared to the textbook relation (Eq. (1), dashed curve). Transmission is in arbitrary units in (b), and fraction transmitted in (c).

Optics EXPRESS

The fabrication begins with the deposition of 5 nm titanium and 60 nm gold by electron beam evaporation on a fused silica substrate. Then, a 570 nm thick layer of silicon dioxide is deposited using plasma-enhanced chemical vapor deposition (PECVD) followed by 300 nm thick layer of amorphous silicon (a-Si). Next, PMMA 950-A2 is spin coated at a speed of 6000 rpm and baked on a hotplate at 180°C for 5 minutes. Electron beam lithography is performed using an Elionix ELS-F125 system operating at 125 kV. The resist is then developed in a mixture of methyl isobutyl ketone and isopropyl alcohol (MIBK:IPA 1:3) at room temperature for 30 s, dipped in IPA for 30 s, and blown dry by nitrogen. Aluminum (Al) is deposited as a mask by thermal evaporation to a thickness of 20 nm. Lift-off is accomplished by soaking the sample in a solvent stripper (Remover PG from Microchem) overnight. Inductively coupled plasma-reactive ion etching (ICP-RIE) is used to etch the a-Si cylinders. In the latter, a gas mixture of SF_6 and CF_4 is used, resulting in highly anisotropic etching of a-Si [43]. Finally the Al mask is removed. Figure 4(a) shows a scanning electron micrograph of a fabricated structure.

Figure 4(b) shows the angle-dependent transmission response. We measure this using a supercontinuum laser (NKT "SuperK") as a tunable light source with a fiber output. The other end of the fiber is connected to an achromatic fiber-coupled collimator, forming a beam with size of 4 mm × 4 mm. The beam then passes through a linear polarizer which is adjusted for s polarization, passed through the sample on a rotation stage, and finally imaged onto a cooled InGaAs camera (Raptor Photonics OW1.7-VS-CL-640).

As we see in Fig. 4(b), the resonant frequency of the cavity shifts by a very small amount as the angle of the incident light changes. It is notable that the shift of the transmission peak is 20 times smaller than the normal expectation from Eq. (1), and with the opposite sign. The shift was not quite zero because of imperfections in the fabrication—see Table 1. (Line "D" in Table 1 corresponds to our measured fabrication results, whereas "A" was our target.) Based on the peak widths, we infer a Q-factor ≥100, instrumentally limited. Asymmetry is evident in both the theoretical and experimental lineshape, indicative of the coupling between the narrow cavity resonance and the relatively broad guided mode resonance [34].

Table 1. Geometric Parameters for Simulations Herein[a]

Structure	Ref.	Cyl. height [nm]	Cyl. diam. [nm]	Cyl. center-to-center spacing [nm]	Cavity thickness [nm]
A	Figures 3(a,e,f,g); Visualization 1	300	490	870	570
B	Figure 3(b)	290	485	965	585
C	Figure 3(c)	510	445	750	360
D	Figure 4(c)	240	495	870	565

[a]Additionally: The gold thickness was 60nm; the SiO_2 refractive index was set to 1.46; the refractive index of amorphous silicon index was based on ellipsometric measurements; and native oxide layers were ignored.

3. Conclusions and future work

We have argued that the phenomena of slow-light or stopped-light waveguides can be mapped into the domain of high-Q planar cavities, thus creating a fascinating platform for physics and engineering. In this preliminary investigation, we have shown that it is possible to create these types of cavities, and given a qualitative overview of the phenomena that result.

While the Q-factors shown here, in the 10^2-10^3 range, are orders of magnitude higher than what has been shown in prior literature [15,22–26], we believe that this approach can be pushed to far higher quality factors in the future, most simply by replacing the metal mirror (which currently limits *Q*) with a better Bragg reflector [27].

There are many further areas to explore in the future, which are beyond the scope of the present work. They include a proper treatment of laser physics, quantum optics, etc., in the context of a laterally-stopped-light resonance; cavity designs for other frequency ranges such

Optics EXPRESS

as far-infrared [44]; and cavity designs with ω_{res} independent of $\mathbf{k}_{xy}$ for both TE and TM modes simultaneously (which would enable more compact modes).

Finally, in the future, a rich area to explore is the addition of lateral variation (non-periodicities) to these types of cavities, bringing them into the realm of *metasurfaces*. A metasurface [45,46] refers generically to a surface in which subwavelength-scale antennas—such as dielectric resonator antennas—alters the phase of light as it passes through the surface. Because most previous work has used weakly-coupled antennas, each emitting mainly dipole radiation, these structures have had phase variation as a function of position, but no appreciable phase variation as a function of angle. The dielectric structure here is the opposite: The reflection phase varies as a function of angle but not of position. A wide variety of new functionalities will be possible by engineering both angle-dependent and position-dependent phase simultaneously.

Appendix

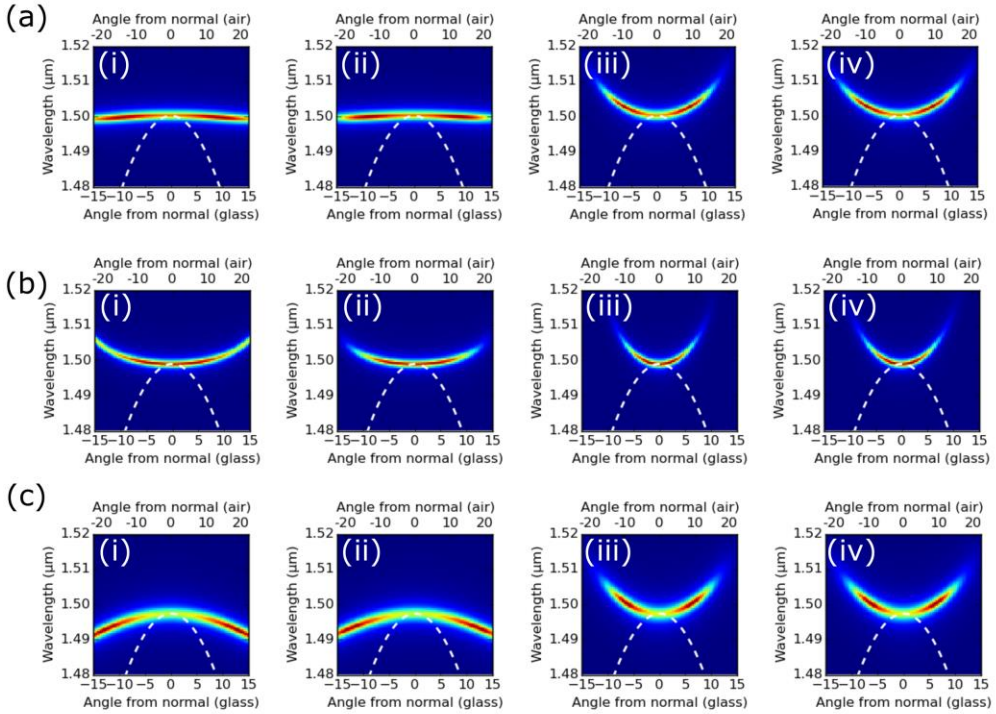

Fig. 5. (a-c) represent the cavities of Fig. 3(a-c) respectively. For each of these, (i) and (ii) are s-polarization light, and (iii) an (iv) are p-polarization, tilted in the two non-equivalent planes of mirror symmetry of the hexagonal lattice.

Funding

Air Force Office of Scientific Research (MURI: FA9550-14-1-0389). Nano-fabrication was performed at the Center for Nanoscale Systems (CNS), a member of the National Nanotechnology Coordinated Infrastructure (NNCI), which is supported by the National Science Foundation under NSF award no. 1541959. CNS is part of Harvard University.

Acknowledgments

The authors acknowledge helpful discussion with T. Mansuripur, M. Kats, R. Devlin, and A. Belyanin.